Imaging of Müllerian Duct Anomalies[1]

Spencer C. Behr, MD • Jesse L. Courtier, MD • Aliya Qayyum, MBBS

ONLINE-ONLY-CME

See www.rsna .org/education /search/RG

LEARNING OBJECTIVES

After completing this journal-based CME activity, participants will be able to:

■ Describe normal embryologic development of the müllerian ducts.

■ Discuss the subtypes of MDAs and differentiation between them.

■ List the potential complications of the various MDA subtypes.

TEACHING POINTS
See last page

The müllerian ducts are paired embryologic structures that undergo fusion and resorption in utero to give rise to the uterus, fallopian tubes, cervix, and upper two-thirds of the vagina. Interruption of normal development of the müllerian ducts can result in formation of müllerian duct anomalies (MDAs). MDAs are a broad and complex spectrum of abnormalities that are often associated with primary amenorrhea, infertility, obstetric complications, and endometriosis. MDAs are commonly associated with renal and other anomalies; thus, identification of both kidneys is important. However, MDAs are not associated with ovarian anomalies. Hysterosalpingography (HSG) is routinely used in evaluation of infertility. Because a key component of MDA characterization is the external uterine fundal contour, HSG is limited for this purpose. Patients suspected of having an MDA are often initially referred for pelvic ultrasonography (US). Magnetic resonance (MR) imaging is typically reserved for complex or indeterminate cases. MR imaging is the imaging standard of reference because it is noninvasive, does not involve ionizing radiation, has multiplanar capability, allows excellent soft-tissue characterization, and permits a greater field of interrogation than does US. Use of MR imaging for evaluation of MDAs reduces the number of invasive procedures and related costs by guiding management decisions.

©RSNA, 2012 • *radiographics.rsna.org*

Introduction

Fusion of the müllerian ducts normally occurs between the 6th and 11th weeks of gestation to form the uterus, fallopian tubes, cervix, and proximal two-thirds of the vagina (1). Any disruption of müllerian duct development during embryogenesis can result in a broad and complex spectrum of congenital abnormalities termed *müllerian duct anomalies* (MDAs). The ovaries and distal third of the vagina originate from the primitive yolk sac and sinovaginal bud, respectively. Therefore, MDAs are not associated with anomalies of the external genitalia or ovarian development.

Diagnosis of MDAs is clinically important because of the high associated risk of infertility, endometriosis, and miscarriage, such that an estimated 15% of women who experience recurrent miscarriages are reported to have MDAs (2). MDAs are also commonly associated with renal anomalies, with a reported prevalence of 30%–50%, including renal agenesis (most commonly unilateral agenesis), ectopia, hypoplasia, fusion, malrotation, and duplication (1,3–5). Other congenital anomalies commonly associated with MDAs include those of the vertebral bodies (29%), such as wedged or fused vertebral bodies and spina bifida (22%–23%), cardiac anomalies (14.5%), and syndromes such as Klippel-Feil syndrome (7%) (6,7).

Buttram and Gibbons (8) proposed an MDA classification in 1979, which was subsequently modified by the American Society for Reproductive Medicine in 1988 (formerly the American Fertility Society) (9). Accurate MDA recognition and classification are critical because treatment varies by the anomaly subtype. Of particular importance is correct identification of a septate uterus, since the septum may be composed predominantly of fibrous tissue; recurrent miscarriage in these patients is attributed to implantation of the embryo onto a poorly vascularized septum. Even with today's state-of-the-art imaging techniques, classification of MDAs may be challenging; when a specific designation cannot be made, it is best to describe the anatomy rather than to force the MDA into a category (1).

Imaging plays an essential role in MDA diagnosis and treatment planning. Currently, magnetic resonance (MR) imaging is the preferred means of evaluation. However, selection of the initial imaging modality is often dictated by the presenting clinical scenario (eg, primary amenorrhea, pelvic pain, or infertility). Hysterosalpingography (HSG) is routinely used in an initial evaluation of infertility; it allows assessment of the uterine cavity and fallopian tube patency but does not provide any information about the external uterine contour.

In younger patients or acute cases, ultrasonography (US) is the preferred method because it is readily available, inexpensive, and rapid and does not use ionizing radiation. Field-of-view restrictions with US, patient body habitus, and artifact from bowel gas may result in a request for further imaging with MR imaging. With the advent of three-dimensional (3D) techniques, US may have the future potential to match the capabilities of MR imaging (10,11). Currently, however, MR imaging remains the preferred MDA imaging method, as it exquisitely details both the uterine cavity and external contours and has shown excellent agreement with clinical MDA subtype diagnosis (12).

In this review, we discuss the embryology and prevalence of MDAs, a classification scheme for MDAs, and MDA imaging methods. In addition, we highlight means to differentiate MDA subtypes and discuss associated anomalies with potential complications.

Embryology

To simplify the embryologic process, we adopted the three-stage approach used by Robbins et al (13): ductal development, ductal fusion, and septal reabsorption.

During the first 6 weeks of development, the male fetus and female fetus are indistinguishable, with both demonstrating paired mesonephric (wolffian or male genital) ducts and paramesonephric (müllerian or female genital) ducts. The presence of a Y chromosome is associated with production of müllerian-inhibiting factor. Therefore, after 6 weeks gestation, the absence of müllerian-inhibiting factor in the female fetus promotes bidirectional growth of the paired müllerian ducts along the lateral aspect of the gonads in conjunction with simultaneous regression of the mesonephric ducts. Interruption of müllerian duct development during this time gives rise to aplasia or hypoplasia of the vagina, cervix, or uterus.

Müllerian duct growth is accompanied by midline migration and fusion of these paired ducts to form the uterovaginal primordium. Interruption of the müllerian duct *fusion* process gives rise to bicornuate uterus and didelphys MDA subtypes.

Between 9 and 12 weeks gestation, the fused müllerian ducts undergo a process of reabsorption of the intervening uterovaginal septum. Interruption of müllerian duct development during this *reabsorption* phase gives rise to septate or ar-
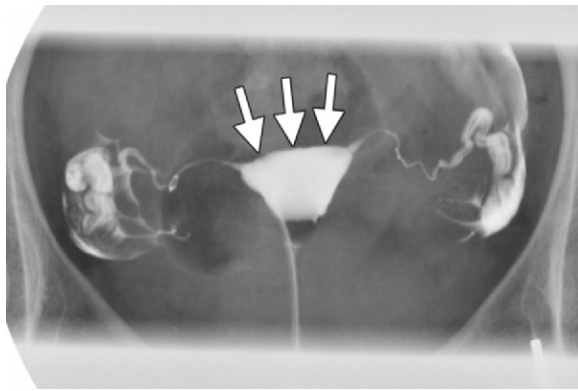
Figure 1. Frontal HSG image shows a normal fundal contour of the endometrial cavity (arrows).

cuate MDA subtypes. The reabsorption process is thought to occur in both cranial and caudal directions (1,14). The bidirectional reabsorption model is more congruent (than the previously suggested unidirectional model) with some forms of MDA such as isolated vaginal septum.

Although interruption in this phase of development is used to explain differences in MDA subtypes, both incomplete müllerian duct fusion and partial reabsorption of the uterovaginal septum may be difficult to differentiate. A common imaging and clinical challenge is the ability to distinguish a bicornuate uterus from a septate uterus. The septate uterus carries a high risk of miscarriage and may be managed with resection of the septum. Absence of a cleft in the external uterine fundal contour with a duplicated endometrial cavity is the key feature used to diagnose a septate uterus rather than a bicornuate uterus.

Prevalence

The reported prevalence of MDA varies widely in the literature, ranging from 1%–5% in the general population (15,16) to 13%–25% among women with recurrent pregnancy loss (15–17). This wide range of reported prevalence may be due to a variety of reasons including, but not limited to, lack of a universal classification system.

In a recent analysis of 94 observational studies, Chan et al (15) reported an MDA prevalence of 5.5% in the general population, 8% in infertile women, 13.3% in women with a history of miscarriage, and 24.5% among women who have experienced miscarriage and infertility. They found that arcuate uterus was most common in the general population, affecting 3.9% of women, followed by bicornuate uterus (0.4%). Among women who experienced challenges conceiving (eg, infertility or miscarriage), septate uterus was a frequent finding, affecting 15.4% of women (15).

Imaging Overview

US and MR imaging play important roles in the diagnosis and evaluation of suspected MDA. HSG is typically indicated in the initial stages of an infertility work-up (18,19). While the presence of a divided rather than triangular uterine cavity at HSG may suggest the presence of an MDA, it is not possible to differentiate between subtypes. MR imaging and US provide greater anatomic detail; both of these imaging methods provide information on the external uterine contour, which is an important diagnostic feature of MDAs. Furthermore, both MR imaging and US may be used to assess for concomitant renal anomalies; renal anomalies occur at a higher rate among MDA patients (3).

Teaching Point

An HSG examination is performed with fluoroscopy; a catheter is placed into the cervical canal, and a balloon is inflated to prevent contrast agent leakage. Water-soluble contrast material is then slowly introduced into the uterine cavity, with select fluoroscopic spot images obtained to evaluate uterine configuration, uterine filling defects, and fallopian tube patency (Fig 1). HSG allows evaluation of only the component of the uterine cavity that communicates with the cervix; since the anatomic information is limited without the ability to evaluate the external contours of the uterine fundus, HSG has little clinical utility in MDA evaluation (1).

US is frequently employed in obstetric and gynecologic evaluations, as it does not require ionizing radiation and is widely available and rapid. Most pelvic US examinations are scheduled after menstruation (days 8–10 of the cycle). During this phase of the cycle, the endometrium is thin. If a diagnosis of MDA is suspected before scheduling the US, it may be advantageous to perform the scan during the latter part of the menstrual cycle, as the thick and highly echogenic appearance of the endometrium during this time may accentuate visualization of the MDA.

The US appearance of a smooth external fundal contour is used to distinguish bicornuate (and didelphys) uteri from septate and arcuate (Fig 2). More recently, 3D US of the uterus (Fig 3) has been reported to improve depiction of the external fundal contour (10,11). Despite such improvements in US technology, significant limitations remain in diagnosing MDA subtypes, including identification of unicornuate uterus and rudimentary uterine horns.

Figure 2. Classification criteria for US differentiation of bicornuate from septate uteri. **(a)** When the apex of the fundal contour is more than 5 mm (arrow) above a line drawn between the tubal ostia, the uterus is septate. **(b, c)** When the apex of the fundal contour is below (arrow in **b**) or less than 5 mm above (arrow in **c**) a line drawn between the tubal ostia, the uterus is bicornuate. (Figs 2a–2c courtesy of Joanna Culley, BA.)
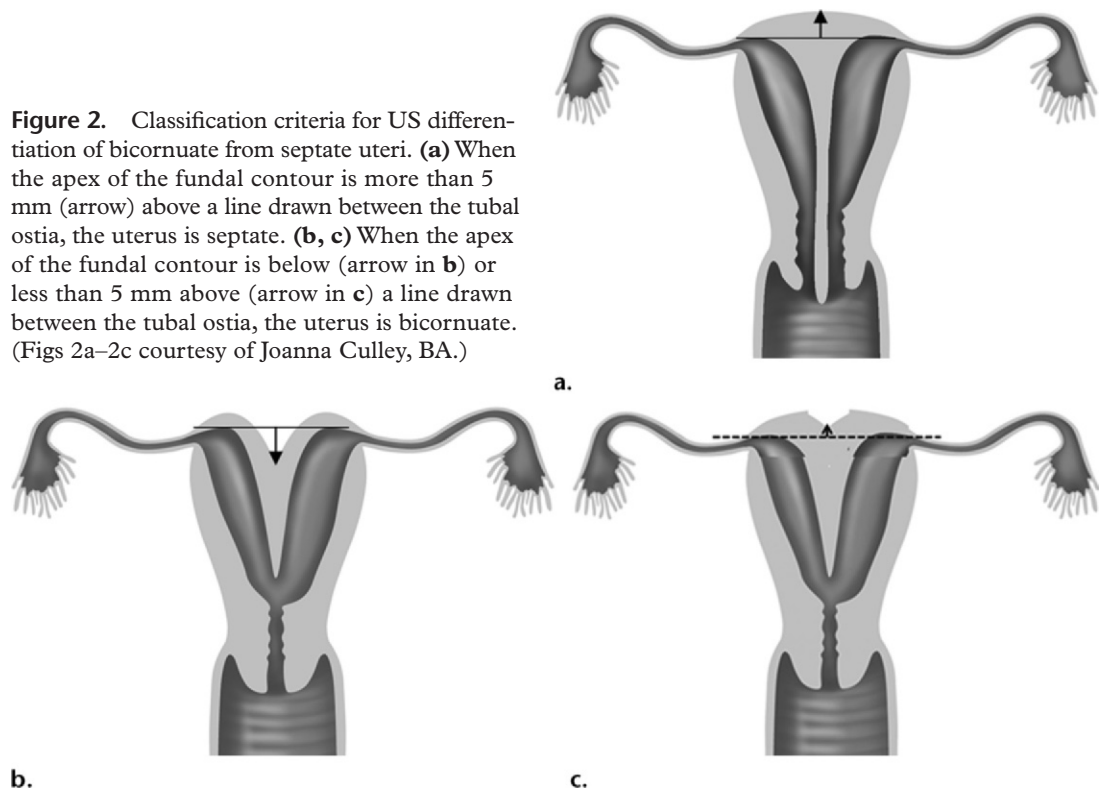

a.

b.

c.

Figure 3. **(a–c)** Multiplanar reconstructions from 3D US show a normal uterus in longitudinal **(a)**, axial **(b)**, and true coronal **(c)** projections. **(d)** Oblique coronal maximum intensity projection reconstructed image in a coronal plane to the uterus show a normal uterine fundal contour.
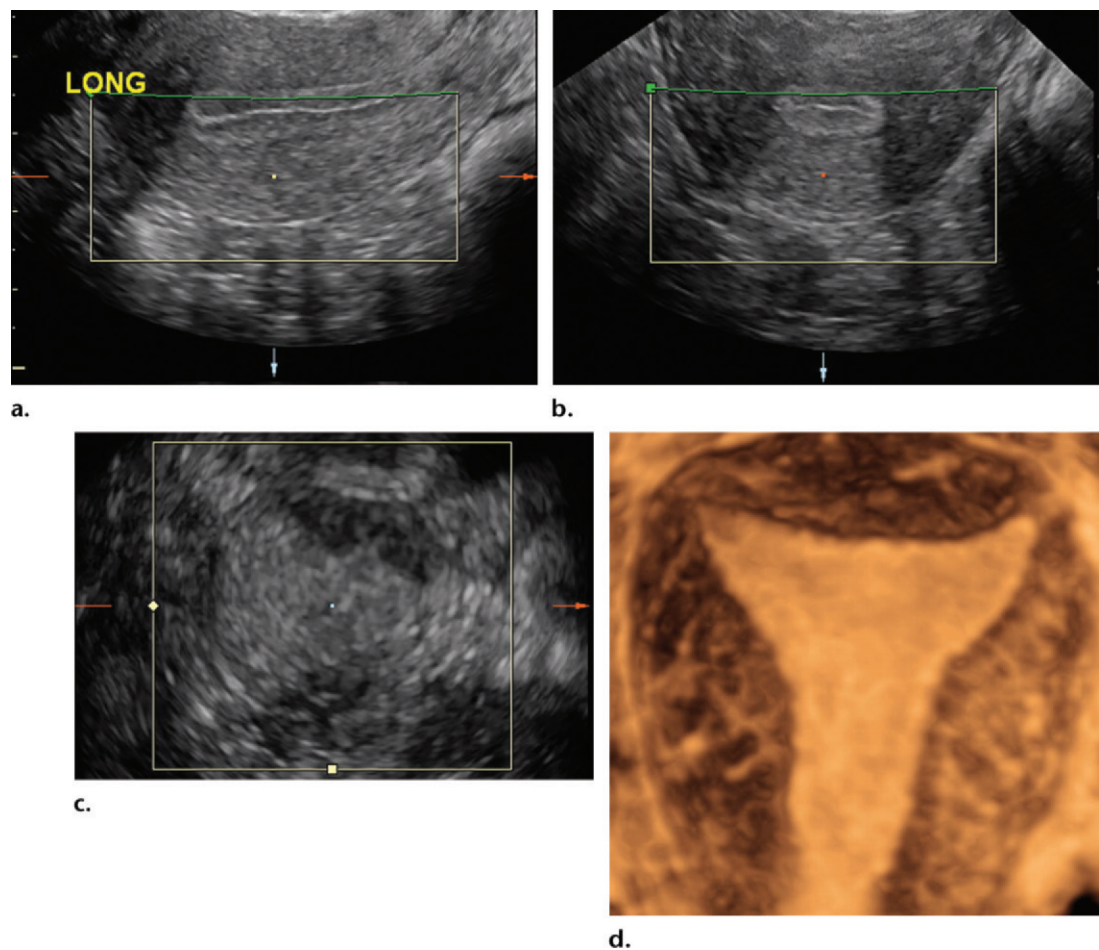

a.

b.

c.

d.

Table 1
MR Imaging Protocol for MDAs

Sequences	Imaging Plane	TR/TE (msec)	Flip Angle (degrees)	NSA	Section Thickness/ Spacing (mm)	Rationale
Routine						
T2W SSFSE	Coronal	1065/865	142	2	5/0	Overview assessment, assessment for renal abnormalities
Dual-echo T1W	Axial	3.66/2.23	12	0.69	5.2/2.6	Short sequence, useful for evaluation of blood products or fat within incidentally found adnexal lesions
3D FS T2W*	Coronal	3748/64.74	90	1	1.4/0.7	Thin-section volumetric acquisition, allows MPR (including coronal images in plane of uterus)
FS T2W motion correction radial blade	Axial	6375/93.63	142	2	4/0	Motion-resistant sequence, particularly useful in younger patients with difficulty staying still
FS T1W volume-interpolated GRE	Axial	2.7/1.3	12	0.7	4/2	Thin-section acquisition, useful for characterization of uterus and adnexal processes
Optional						
FS T2W FSE	Oblique coronal	3150/36.1	90	2	4/0	Can be performed as supplement or adjunct to 3D T2W reformatted images in plane of uterus
Dynamic† CE FS T1W volume-interpolated GRE	Axial or sagittal per physician	2.7/1.3	12	0.7	4/2	Performed if additional characterization of incidentally seen disease is necessary
CE FS T1W volume-interpolated GRE	Coronal	2.7/1.3	12	0.7	4/2	Delayed imaging may be useful for assessment of distal ureter if anomalous ureteral insertion is suspected

Note.—Routine 3-T MR imaging sequences for evaluation of the female pelvis at our institution. The clinical situation dictates use of the optional sequences. CE = contrast-enhanced, FS = fat-saturated, FSE = fast spin-echo, GRE = gradient-echo, MPR = multiplanar reformatting, NSA = number of signals acquired, SSFSE = single-shot FSE, TE = echo time, T1W = T1-weighted, TR = repetition time, T2W = T2-weighted.
*Technologist to generate axial, sagittal, and oblique coronal reformatted images.
†Phases at 30, 60, and 90 seconds and 3 minutes.

MR imaging is considered the ideal imaging modality for evaluation of MDAs. MR imaging provides clear anatomic detail of both the internal uterine cavity and the external contour. Standard pelvic MR imaging protocols (Table 1) include axial T1-weighted and T2-weighted images (T2-weighted imaging is essential for evaluation of uterine anatomy). Contrast material is generally reserved for assessment of incidentally discovered additional disease.

For the purpose of MDA classification, oblique coronal T2-weighted images of the uterus are the most critical, since these are necessary for proper assessment of the uterine fundal contour. Newer 3D T2-weighted sequences provide submillimeter section thickness along with multiplanar reformatting capability. The advantage
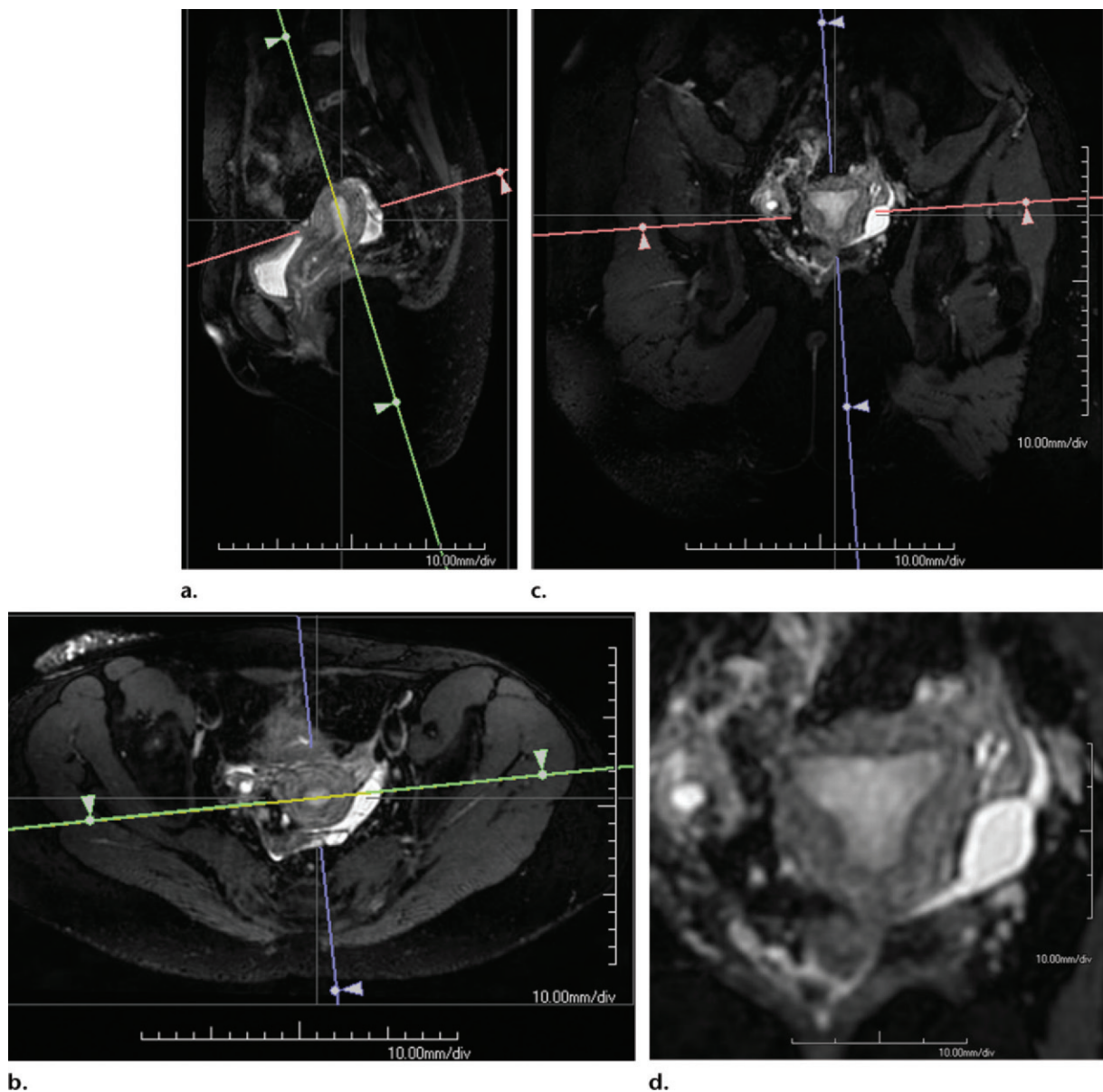
Figure 4. **(a–c)** Multiplanar reconstructions from 3D T2-weighted MR imaging show a normal uterus in sagittal **(a)**, axial **(b)**, and true coronal **(c)** projections of the pelvis. **(d)** Oblique coronal reconstructed image in a coronal plane to the uterus shows normal uterine fundal contour.

of multiplanar reformatting is that it significantly reduces imaging time (particularly important in pediatric and sedated or anesthetized patients) and avoids the need for exact prescription of the imaging plane, since this can be performed retrospectively at the workstation (Fig 4).

Concomitant renal anomalies are reported in 29% of MDA cases (3). Therefore, it is important to examine the kidneys at cross-sectional imaging (US and MR imaging) performed for MDA. The spectrum of renal anomalies includes agenesis, horseshoe kidney, renal dysplasia, ectopic kidney, and duplicated collecting systems (20).
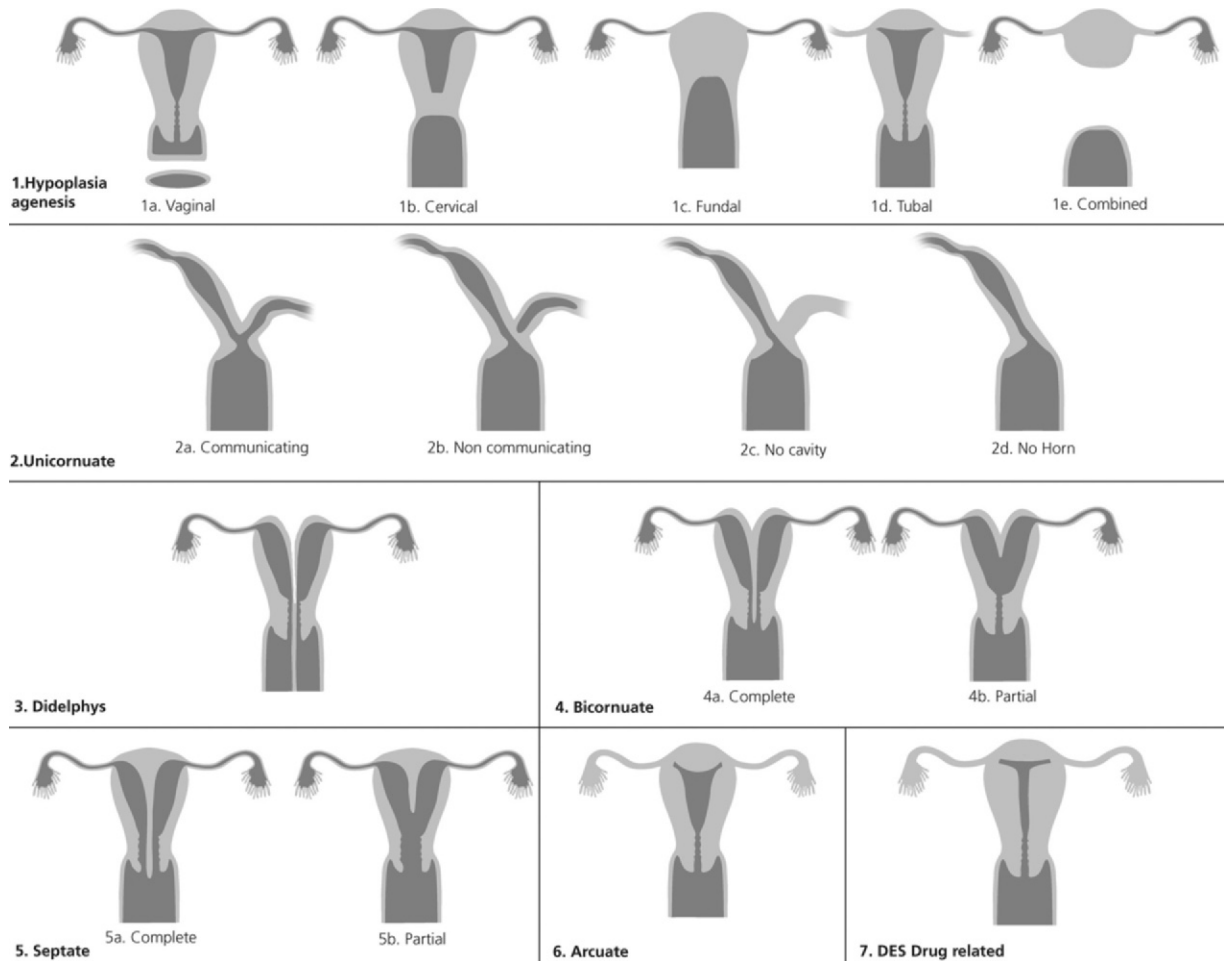
Figure 5.   Classification of MDAs on the basis of the American Society for Reproductive Medicine system. *DES* = diethylstilbestrol. (Courtesy of Joanna Culley, BA.)

Classification

There is no universally accepted MDA classification system; each system has its shortcomings. However, the system proposed by Buttram and Gibbons (8) in 1979 and subsequently revised by the American Society for Reproductive Medicine in 1988 (9) is the most widely accepted (Fig 5). The limitation of the Buttram and Gibbons (8) classification system is its lack of categorization of vaginal and other anomalies that bridge more than one classification (1,14). In these situations, it is best to describe each anomaly in detail, as confusion may arise from a forced classification fit (1,14).

Agenesis or Hypoplasia

General Information.—Early developmental failure of the müllerian ducts results in agenesis or hypoplasia of the proximal two-thirds of the vagina, cervix, and uterus. This anomaly is part of the Mayer-Rokitansky-Küster-Hauser syndrome (Fig 6) and represents the most extreme form of MDA: complete agenesis of the proximal vagina, cervix, and uterus. Clinical presentation occurs at puberty with primary amenorrhea (1). In the setting of isolated partial vaginal agenesis and a
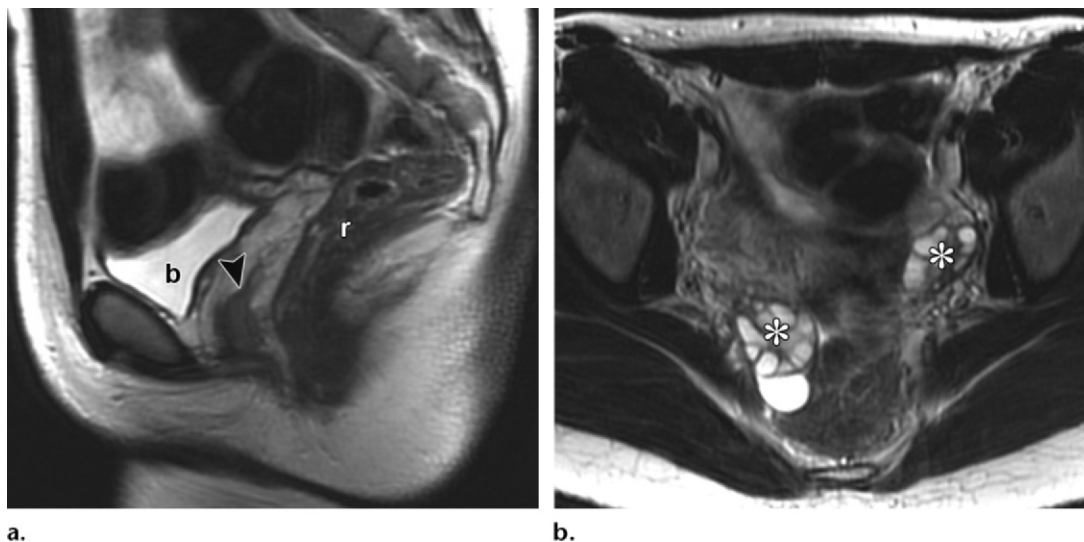
Figure 6.   Mayer-Rokitansky-Küster-Hauser syndrome. **(a)** Sagittal T2-weighted MR image shows complete absence of the cervix and uterus with an abnormally truncated vagina ending in a blind pouch (arrowhead) between the rectum *(r)* and urinary bladder *(b)*. **(b)** Axial T2-weighted image shows the presence of normal ovaries (∗).

normal uterine cavity, patients may present with primary amenorrhea in conjunction with hematometra or cyclic pelvic pain that may require surgical intervention (21).

The primary aim of treatment for women with müllerian agenesis is to enable normal sexual function through creation of a neovagina. Techniques employed include use of dilation devices to gradually lengthen and stretch the vagina. More severe cases may be treated surgically by using the McIndoe procedure or sigmoid vaginoplasty. Imaging may be helpful in preoperative evaluation. Success of the McIndoe procedure requires an adequate space between the rectum and bladder, placement of a split-thickness skin graft, and stent placement in the neovagina during the healing process (7).

Imaging Findings.—HSG has no role in evaluation of müllerian agenesis or hypoplasia, and initial imaging is typically with US. Expected US findings include normal-appearing ovaries without identification of a normal uterus. However, confident diagnosis of uterine agenesis or hypoplasia may be difficult, especially given that the uterus location is variable (22–24).

MR imaging is ideal for investigating primary amenorrhea with respect to differentiating uterine hypoplasia or agenesis from other causes of primary amenorrhea, such as androgen insensitivity syndrome, which is seen in association with rudi-

mentary testes. A further important advantage of MR imaging is the ability to readily evaluate the patient for concurrent renal anomalies, reported to occur in approximately 40% (30%–50%) of patients with MDAs (23).

The anatomy of the female reproductive tract is best seen on T2-weighted images. T1-weighted imaging is useful for identification of high-signal-intensity blood products as a diagnostic feature of endometriosis. Sagittal T2-weighted sequences are particularly helpful when attempting to determine a diagnosis of uterine agenesis or hypoplasia, since the expected location of the vagina, cervix, and uterus may be extrapolated from the location of the bladder, urethra, and lower vagina. In the presence of complete uterine agenesis, there is no identifiable uterus. A hypoplastic uterus may be seen as a soft-tissue pelvic mass with signal intensity characteristics of normal myometrium (slightly hyperintense on T2-weighted images).

The myometrium of the rudimentary uterus is affected by the presence of circulating female hormones, and it may even be possible to identify zonal anatomy. Before puberty, the myometrium is hypointense on T2-weighted images and demonstrates poorly defined zonal anatomy. After the onset of puberty, the signal intensity of the myometrium on T2-weighted images increases and zonal anatomy becomes evident. In cases of isolated vaginal agenesis, the length of the atretic vaginal segment may influence surgical approach and is optimally determined in the sagittal plane (21).
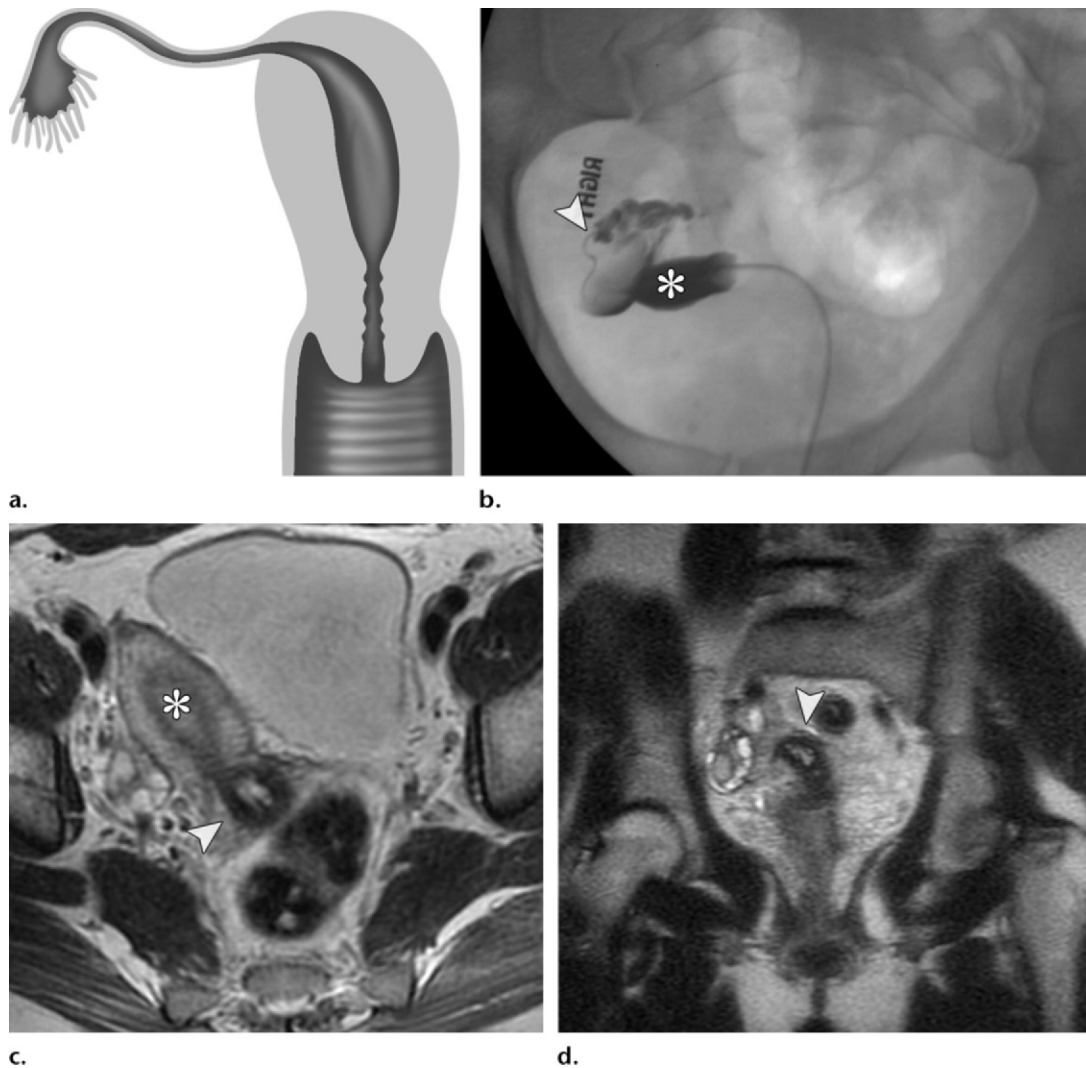
Teaching Point

Figure 7.   Unicornuate uterus with no rudimentary horn. **(a)** Illustration shows a right unicornuate uterus with no rudimentary horn. **(b)** HSG image shows a small, oblong uterine cavity (∗) deviated to the right of midline with a single fallopian tube (arrowhead). **(c)** Axial T2-weighted MR image shows a single uterine horn (∗) and cervix (arrowhead). **(d)** Coronal T2-weighted MR image shows absence of soft tissue adjacent to the right unicornuate cervix (arrowhead), a finding indicating absence of a rudimentary horn. (Fig 7a courtesy of Joanna Culley, BA.)

Unicornuate Uterus

***General Information.*—**A unicornuate uterus results from normal development of one müllerian duct and near complete to complete arrested development of the contralateral duct. This anomaly has four potential subtypes: *(a)* no rudimentary horn (Fig 7), *(b)* rudimentary horn with no uterine cavity, *(c)* rudimentary horn with a communicating cavity to the normal side, and *(d)* rudimentary horn with a noncommunicating cavity. Approximately 40% of unicornuate uteri have renal anomalies ipsilateral to the rudimentary horn, with renal agenesis being the most common (67% of cases) (3).

A rudimentary horn without endometrium and the absent rudimentary horn subtype present minimal risk and do not usually require surgical intervention. However, the presence of endometrium in a rudimentary horn is an important finding and should be reported. Endometrial tissue in a noncommunicating rudimentary horn can manifest clinically with pelvic pain caused by the increased prevalence of endometriosis due to retrograde flow of menses through the obstructed horn or due to an obstructed, distended horn (Fig 8) (25,26). In addition, the presence of endometrium in a rudimentary
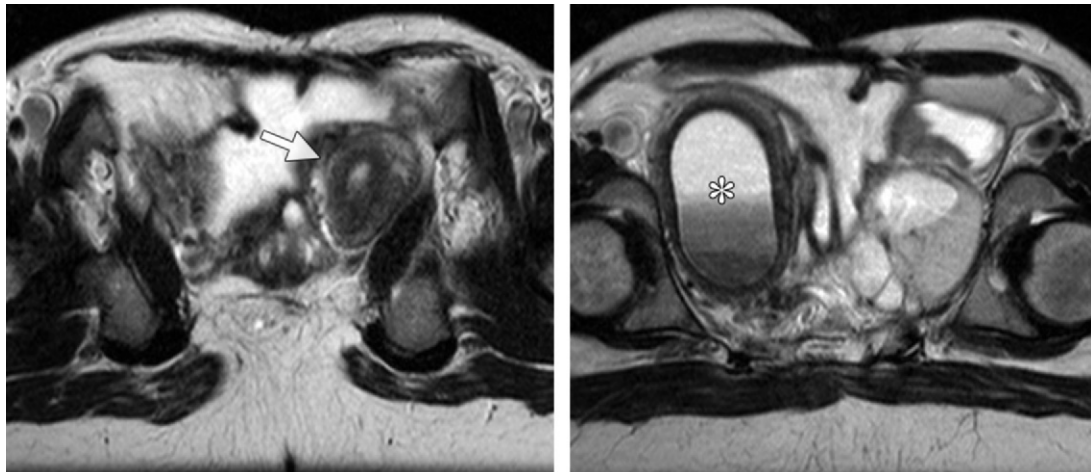
Teaching Point

Figure 8. Unicornuate uterus with an obstructed noncommunicating rudimentary horn. Axial T2-weighted MR images show a normal-appearing left unicornuate uterus (arrow in **a**) and an obstructed noncommunicating right rudimentary horn with layering debris (∗ in **b**).
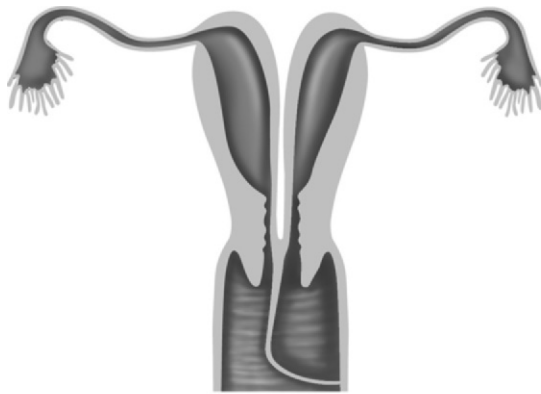

Figure 9. Uterus didelphys. **(a)** Illustration shows a uterus didelphys with a left transverse vaginal septum. **(b)** Coronal T2-weighted image of a uterus didelphys, obtained in plane with the uterus, shows two widely divergent uterine horns (arrows) separated by a deep fundal cleft. Two separate cervices are present (arrowheads). **(c)** Axial image caudal to **b** shows two vaginas (arrows). (Fig 9a courtesy of Joanna Culley, BA.)
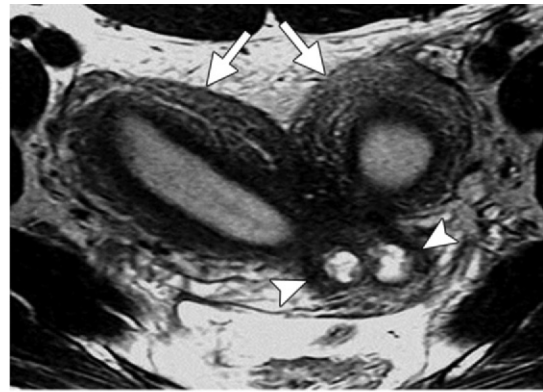
horn, whether or not it communicates with the uterine cavity, carries an increased risk of miscarriage, ectopic pregnancy, preterm labor, and, most significantly, uterine rupture (27).

Imaging Findings.—At HSG (Fig 7b), an off-midline fusiform uterine cavity is seen with contrast opacification of a solitary fallopian tube. While a communicating rudimentary uterine horn may be visualized, HSG cannot be used to exclude the presence of a noncommunicating rudimentary horn (28,29).

At US, the unicornuate uterus may appear as a small, oblong, off-midline structure. The rudimentary horn is often hard to identify and may be misdiagnosed as a pelvic mass or the cervix (1,11).

At MR imaging (Fig 7c, 7d), the small, curved unicornuate uterus is typically displaced off midline. It has normal myometrial zonal anatomy, with normal endometrial-to-myometrial width and ratio (30,31). The appearance of
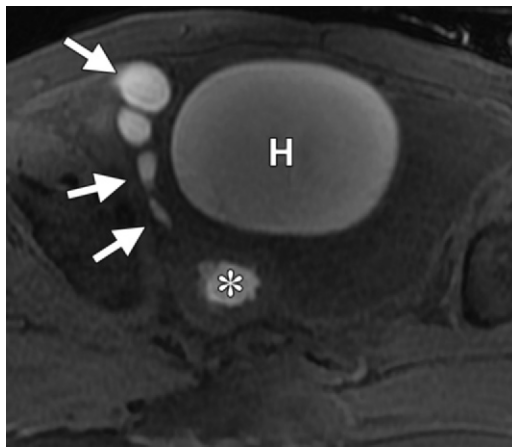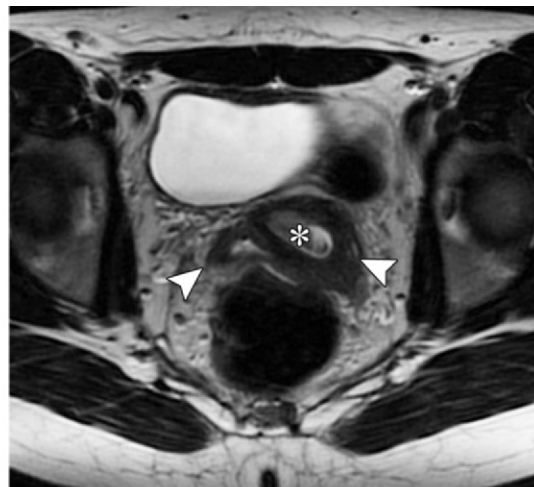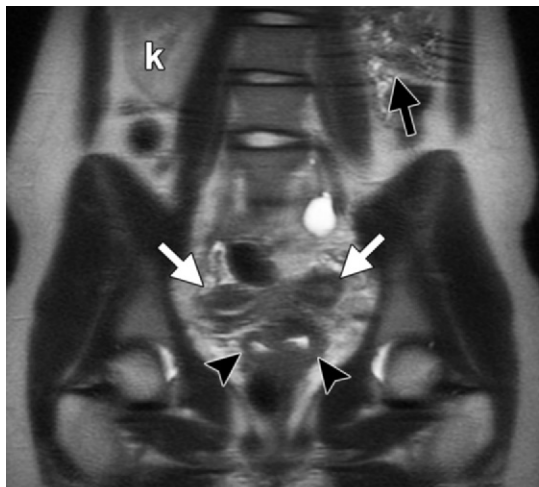
Figure 10.   Axial spoiled gradient-echo fat-saturated T1-weighted MR image shows hyperintense blood products within an obstructed horn of a uterus didelphys (∗). The hyperintense blood products decompress through the fallopian tube (arrows) into a large hematosalpinx *(H)*.

a.   b.

Figure 11.   Uterus didelphys with an obstructed hemivagina. **(a)** Coronal single-shot fast spin-echo T2-weighted MR image shows widely separated horns of a uterus didelphys (white arrows). Two hemivaginas are present (arrowheads). Note the absent left kidney (black arrow) with bowel in the renal fossa, which is ipsilateral to the obstructed hemivagina. *k* = normal right kidney. **(b)** Axial T2-weighted image shows the two hemivaginas (arrowheads); the obstructed, dilated left hemivagina contains heterogeneous debris (∗).

the rudimentary horn varies by subtype. If there is no endometrium present, zonal anatomy is absent and the entire horn may demonstrate diffuse low signal intensity.

If endometrial tissue is present, there may be preserved zonal anatomy, and the rudimentary horn may become distended with blood products after onset of menarche if there is no communication with the fully developed uterine horn. A noncommunicating rudimentary horn with endometrium may manifest as a large uterine mass and endometriosis requiring surgical intervention (1).

Uterus Didelphys

General Information.—Uterus didelphys results from complete failure of müllerian duct fusion.

Each duct develops fully with duplication of the uterine horns, cervix, and proximal vagina (in three-fourths of patients) (32) (Fig 9).

A duplicated (proximal) vagina may be associated with a transverse hemivaginal septum, resulting in ipsilateral obstruction and hematometrocolpos (1) (Fig 10). In the absence of vaginal obstruction, uterus didelphys is usually asymptomatic. Patients with hemivaginal obstruction present with dysmenorrhea secondary to endometriosis, infections, and pelvic adhesions attributed to retrograde menstrual flow from the obstructed side (25,26). With respect to renal anomalies, an obstructed uterus didelphys is commonly associated with ipsilateral renal agenesis (3) (Fig 11).

Imaging Findings.—HSG demonstrates two separate, oblong endometrial cavities with contrast opacification of fallopian tubes. The presence of an obstructed transverse septum may result in nonopacification of the ipsilateral uterine horn and is a potential pitfall leading to the misdiagnosis of unicornuate uterus (33,34).

At US, the differentiation of fusion (didelphys and bicornuate) anomalies from reabsorption (septate and arcuate) anomalies is based on the presence of a uterine fundal cleft (Fig 2). To best demonstrate the cleft, a true coronal image oriented to the uterine fundus should be obtained. In uterus didelphys, the two uterine horns are widely divergent with separate, noncommunicating endometrial cavities (Fig 12). Identification of two cervices and duplicated upper vaginas should be documented (1). Duplication of the vagina (hemivaginal septum) may not be apparent; in such circumstances, the distinction between uterus didelphys and a bicornuate bicollis uterus may be difficult.

As with US, MR imaging demonstrates two widely divergent uterine horns and two separate cervices. A fundal cleft greater than 1 cm has been reported to be 100% sensitive and specific in differentiation of fusion anomalies (didelphys and bicornuate) from reabsorption anomalies (septate and arcuate) (35) (Fig 9b, 9c). Although measurements are often reported in the literature, from a practical perspective identification of a clefted external fundal contour is most commonly used.

In uterus didelphys, the endometrial-to-myometrial ratio as well as the zonal anatomy are normal (30,31,35). Duplication of the proximal vagina may be visualized at MR imaging, and this may be further improved by instillation of viscous liquid, such as ultrasound gel, into the vagina before imaging. The presence of a unilateral hemivaginal septum obstructing one of the uterine horns will cause that horn to be markedly distended from blood products, demonstrating high signal intensity at T1-weighted imaging.

Bicornuate Uterus

General Information.—Bicornuate uterus results from incomplete or partial fusion of the müllerian ducts and accounts for approximately 10% of MDAs (1). Bicornuate uterus is characterized by the presence of a cleft (>1 cm in
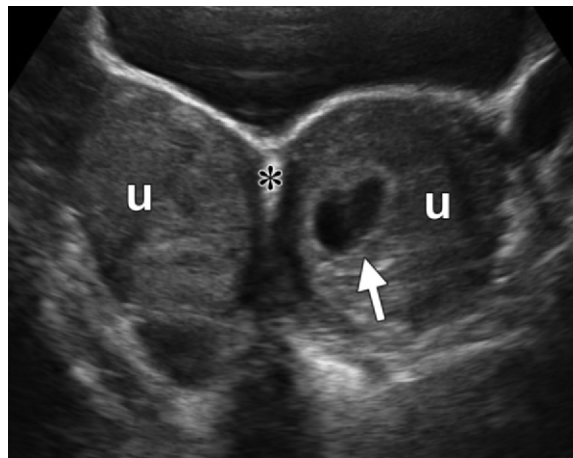

Figure 12. Transverse transabdominal US image shows a uterus didelphys, with two uterine horns *(u)* separated by echogenic fat (∗). There is a viable embryo (arrow) in the left uterine horn.

depth at MR imaging) in the external contour of the uterine fundus, similar to uterus didelphys. The duplicated endometrial cavity may be associated with cervix duplication (bicornuate bicollis) or be without cervix duplication (bicornuate unicollis) (Fig 13). If a longitudinal vaginal septum is also present (one-fourth of cases), a bicornuate bicollis uterus may be indistinguishable from a uterus didelphys.

Surgical intervention is not usually indicated for patients with bicornuate uterus, since they are often asymptomatic. That said, if a patient presents with hematocolpos or dyspareunia, a vaginal septoplasty is indicated (21,36).

Imaging Findings.—HSG demonstrates opacification of two symmetric fusiform uterine cavities (horns) and fallopian tubes. Historically, an intercornual angle of greater than 105° was used for diagnosis. However, imaging overlap with a septate uterus makes differentiation impossible at HSG examination (31,33,34).

MR imaging (Fig 13c) and US (Fig 13d) should be used to identify the presence of a deep fundal cleft (see discussion on septate uterus in the next section). At US, divergent uterine horns and separation of uterine cavities may be optimally seen in the secretory phase of the menstrual cycle due to echogenicity of the endometrium. At MR imaging, both uterine horns have normal zonal anatomy. The appearance of a duplicated cervix ("owl eyes") is seen in patients with a bicornuate bicollis uterus, which can be confidently diagnosed in the absence of vaginal duplication.
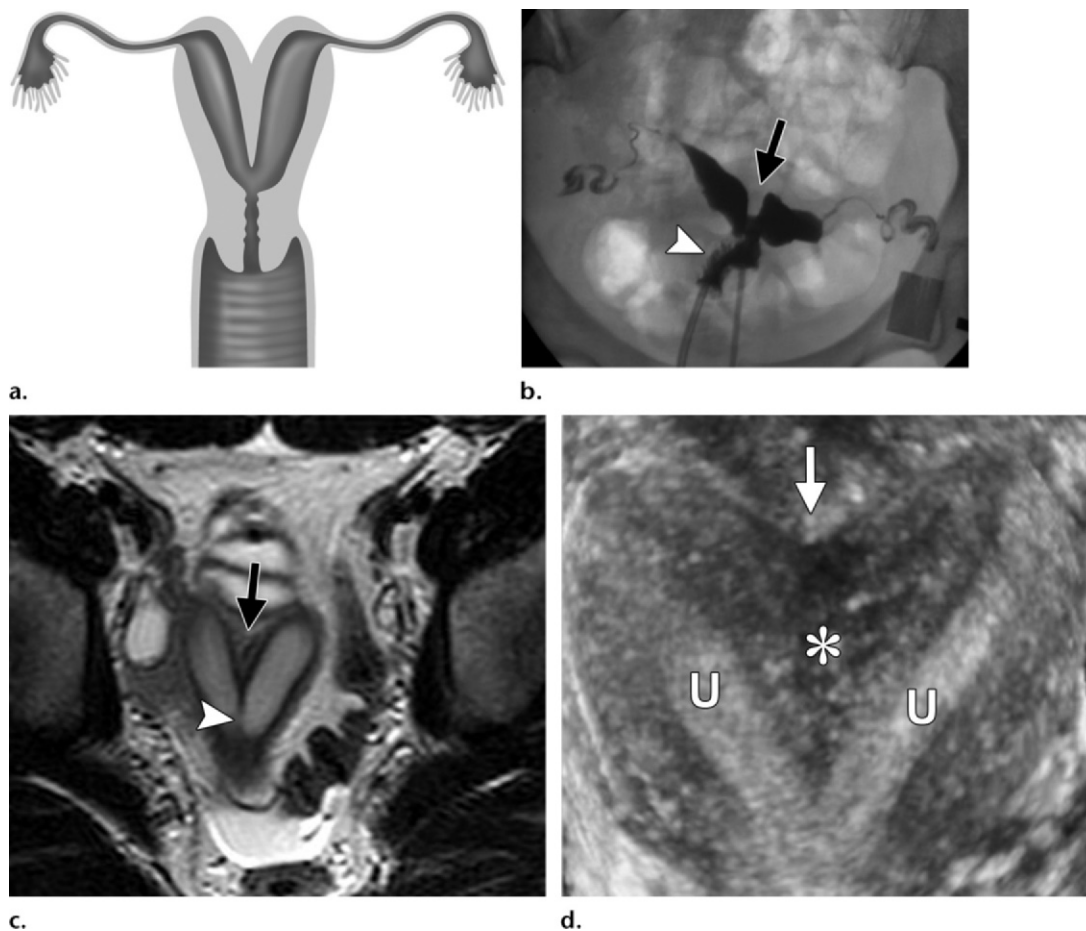
Figure 13. Bicornuate uterus. **(a)** Illustration shows a bicornuate unicollis uterus. **(b)** HSG image shows a bicornuate bicollis uterus with two HSG cannulas due to two cervices. There is a fundal linear defect (arrow) with filling of two symmetric uterine horns through the right cannula (arrowhead) due to communication in the lower uterine segment. **(c)** Axial T2-weighted MR image shows a uterine fundal cleft (arrow) greater than 1 cm with soft tissue separating the two symmetric uterine cavities. This finding is critical for distinction from uterus didelphys. Arrowhead = communication between the two cavities. **(d)** Coronal 3D US image shows the prominent uterine fundal cleft (arrow), which represents the presence of a fusion anomaly, and uterine fundal soft tissue (∗) separating into the symmetric uterine cavities *(U)*, which communicate at the level of the uterine isthmus. (Fig 13a courtesy of Joanna Culley, BA.)

Septate Uterus

General Information.—Septate uterus is the most common form of MDA, accounting for approximately 55% of cases (37–39). A septate uterus may be suspected in patients with a history of midtrimester pregnancy loss (39,40). Correct diagnosis is important because a septate uterus is surgically correctable and has a strong association with repeated miscarriage. The most common diagnostic dilemma encountered in patients suspected of having an MDA is inability to differentiate between a septate and bicornuate uterus. As discussed earlier, the primary difference is the appearance of the uterine

fundus; a septate uterus will have a normal convex external fundal contour (Fig 14).

The septum itself originates from the midline of the uterine fundus and is a result of complete or partial failure of reabsorption of the uterovaginal septum. The septum may be partial or complete. A complete septum extends to the external cervical os and may even extend into the vagina in approximately one-fourth of patients (41). The septum may be of variable length and tissue composition, consisting of varying proportions of fibrous tissue and myometrium (30,31,42).
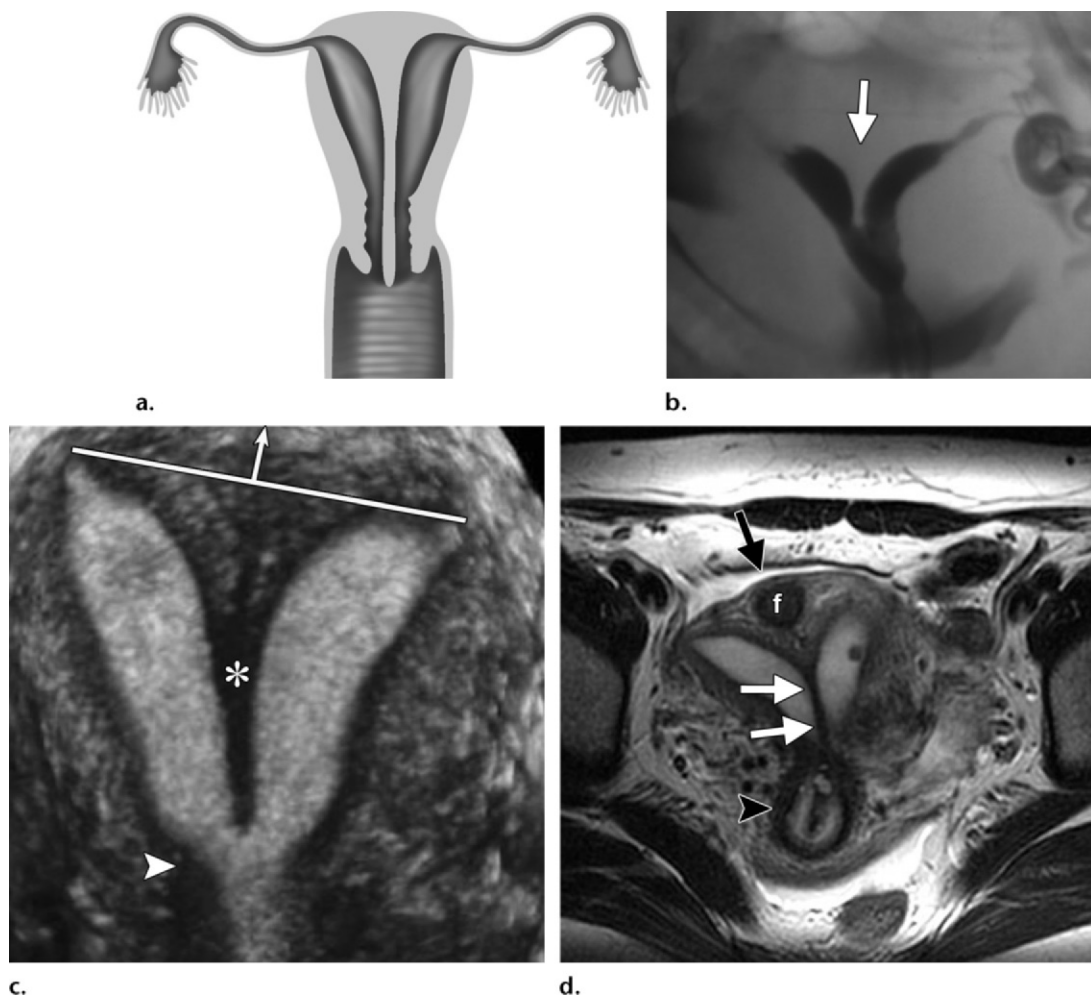
Figure 14. Septate uterus. **(a)** Illustration shows a complete septate uterus. **(b)** HSG image of a partial septate uterus shows a thin linear filling defect (arrow) extending from the uterine fundus, separating the uterine cavity into two symmetric cavities. **(c)** Coronal 3D US image of a partial septate uterus shows the isoechoic muscular septum and hypoechoic fibrous septum (*), which extends just proximal to the internal cervical os (arrowhead). The apex of the fundal contour (arrow) is more than 5 mm above a line drawn between the tubal ostia (white line), a finding compatible with a septate uterus. **(d)** Axial T2-weighted MR image of a complete septate uterus shows a normal external uterine contour (black arrow). The hypointense fibrous septum (white arrows) originates from the isointense muscular septum and extends into the cervical os (arrowhead). A hypointense uterine fundal fibroid *(f)* is also present. (Fig 14a courtesy of Joanna Culley, BA.)

Imaging Findings.—HSG (Fig 14b) cannot be used to evaluate the external uterine contour and therefore does not allow reliable differentiation of septate from bicornuate uterus (43). Historically, an angle of less than 75° between the uterine horns is reported to be suggestive of a septate rather than bicornuate uterus (33,43). However, considerable overlap occurs in the angle measurements between septate and bicornuate uteri; as such, the angle measurement is not a reliable diagnostic feature (1).

US features suggestive of a septate uterus include interruption of the myometrium by a septum at the fundus (Fig 14c). The fibrous component of the septum is less echogenic relative to myome-

trium. Although 3D US may improve assessment of the external uterine contour compared with 2D imaging, a confident diagnosis is frequently difficult (10,11). The true orthogonal plane to the long axis of the uterus should be used.

A line drawn between the uterine ostia (Fig 2) may be used to differentiate between a septate and bicornuate uterus. In a septate uterus, the apex of the external fundal contour is more than 5 mm above the interostial line. By comparison, in a bicornuate or didelphys uterus, the apex of the external fundal contour is below or less than 5 mm above the interostial line (1,37,44).

At MR imaging, the uterus is normal in size. Again, the key to differentiating a septate uterus from a bicornuate uterus is the external fun-
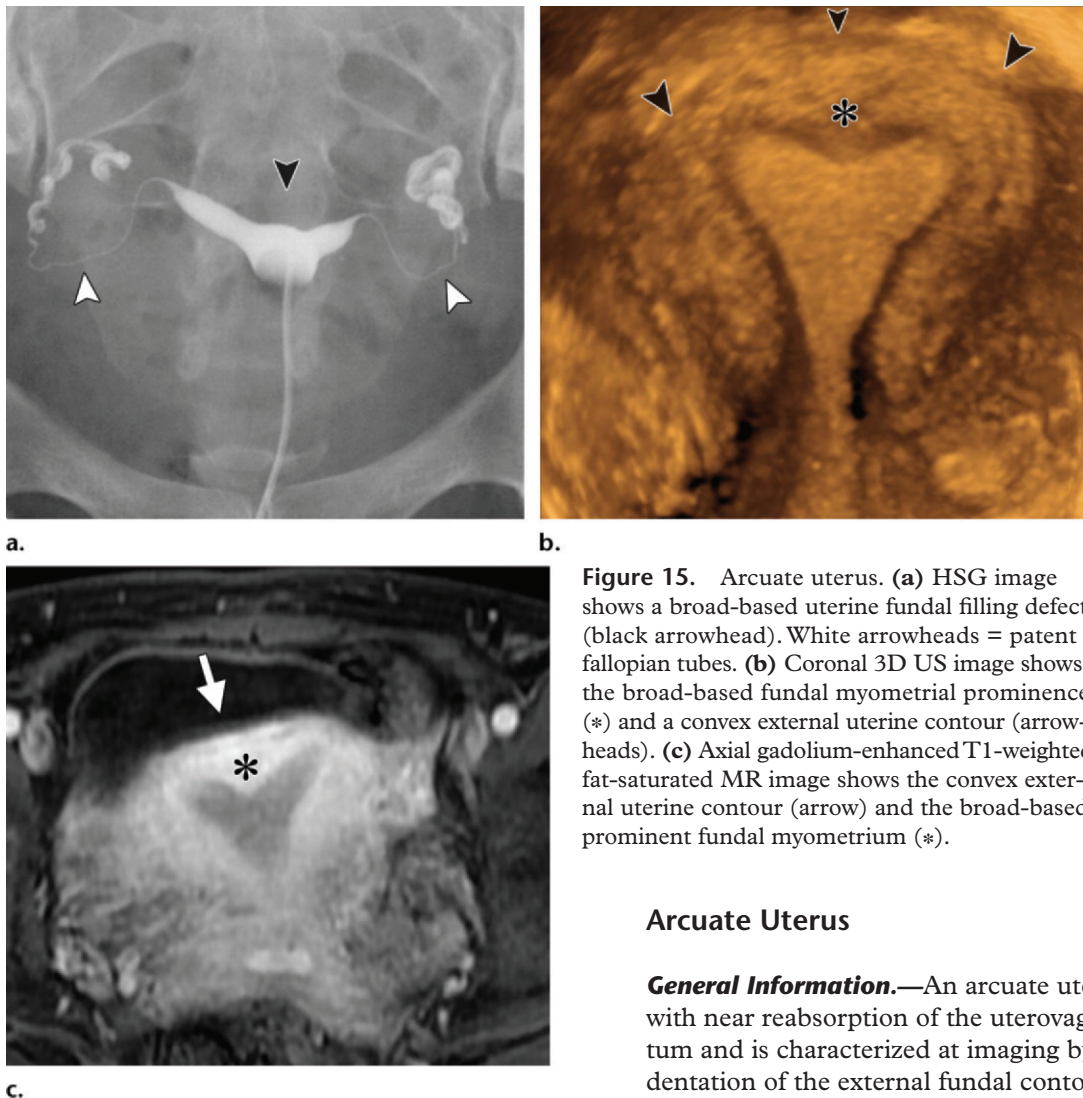
a.

b.

c.

Figure 15. Arcuate uterus. **(a)** HSG image shows a broad-based uterine fundal filling defect (black arrowhead). White arrowheads = patent fallopian tubes. **(b)** Coronal 3D US image shows the broad-based fundal myometrial prominence (∗) and a convex external uterine contour (arrowheads). **(c)** Axial gadolium-enhanced T1-weighted fat-saturated MR image shows the convex external uterine contour (arrow) and the broad-based prominent fundal myometrium (∗).

Arcuate Uterus

General Information.—An arcuate uterus occurs with near reabsorption of the uterovaginal septum and is characterized at imaging by a mild indentation of the external fundal contour (Fig 15). Buttram and Gibbons (8) originally classified arcuate uterus as a subclass of bicornuate uterus. Later, the American Society for Reproductive Medicine established a separate classification in view of the normal external fundal contour (9).

In general, this is considered a mild form of MDA and is typically associated with normal-term gestation (45). However, surgical correction might be considered in cases of repeat pregnancy loss (1).

Imaging Findings.—At HSG, a single uterine cavity with a broad saddle-shaped indentation at the uterine fundus is seen (31) (Fig 15a). Similarly, on US images a broad, smooth inward contour deformity of the uterine fundus is seen (Fig 15b). There is a normal external contour.

At MR imaging, there is a normal-sized uterus, and the normal convex external uterine fundal contour is maintained (Fig 15c). There is a broad-based, smooth prominence of soft tissue at the fundus with indentation of the endometrial

dal contour (Fig 14d). The presence of a clear fundal cleft is a highly reliable indicator for fusion anomalies such as bicornuate uterus rather than reabsorption anomalies (septate or arcuate uterus) (35).

T2-weighted images readily demonstrate the presence of high-signal-intensity myometrium (generally seen closer to the fundus in patients with a complete septum) and a low-signal-intensity fibrous septum, which may extend to the external cervical os (31,42). It is important to identify myometrium versus fibrous tissue within the septum, since the surgical approach differs for the two entities; while a less invasive hysteroscopic septoplasty can be used to treat a fibrous septum, a transabdominal surgical approach is required for treatment of a muscular septum (20).

Rarely, duplication of the cervix can also be seen in patients with a complete septate uterus (1). The potential pitfall of misdiagnosis as a bicornuate bicollis uterus is avoided through careful interrogation of the external uterine contour.

Teaching Point

cavity. The T2-weighted signal intensity of the soft-tissue prominence is consistent with myometrium without demonstration of fibrous tissue (low signal intensity on T2-weighted images).

DES Uterus

General Information.—DES-related anomaly of the uterus involves a hypoplastic or T-shaped uterus, which is now more of historical interest. DES is a synthetic nonsteroidal estrogen that was used to prevent miscarriage in high-risk patients during the late 1940s to 1971. Prescription of DES was stopped in the 1970s after an article in the *New England Journal of Medicine* linked in utero DES exposure with vaginal clear cell carcinoma and uterine, cervical, and vaginal malformations (46).

Features of a T-shaped uterus include a widened lower uterine segment, a small hypoplastic uterus, a narrowed fundal endometrial canal, irregular endometrial margins, and intraluminal uterine filling defects (47,48). Cervical anomalies include hypoplasia, anterior cervical ridge, cervical collar, and pseudopolyposis (47–49). Fallopian tube anomalies include a truncated appearance, saccular outpouchings, and fimbria deformities (50).

An interesting point is that the spectrum of anomalies noted among DES-exposed patients has also been noted—albeit rarely—among women without DES exposure (51). This suggests that this configuration is not caused by DES exposure alone but may have additional origins (1).

Imaging Findings.—At HSG, a DES uterus demonstrates the classic T-shaped configuration (Fig 16); it is reported to occur in 31% of exposed women (47,48). The T-shaped appearance is secondary to the shortened upper uterine segment (1). The fallopian tubes are often truncated and have an irregular appearance (33,50–52). In addition, constriction bands at the midfundal segment may be present, which leads to narrowing of the proximal fallopian tube (1).

As in other subtypes of MDA, 2D US features are nonspecific; thus, obtaining a specific diagnosis with this imaging modality is not possible (52,53).

At MR imaging, the hypoplastic uterus is seen to have an abnormal T-shaped endometrial configuration and demonstrates constriction bands (1), which are described as focal junctional zone thickening resulting in a narrowed and irregular appearance of the endometrial cavity (54).

Conclusions

MDAs are a complex and broad spectrum of developmental anomalies that can manifest in a va-

Figure 16. DES uterus. HSG image shows the classic T-shaped uterine cavity due to DES exposure.

riety of both clinical and imaging scenarios. While MDAs may be initially detected at HSG during investigation of infertility or at US, MR imaging is currently the imaging modality of choice due to its reliability and accuracy. On identification of an MDA, radiologists should also look for associated renal and skeletal anomalies. Anomalies of the renal tract may be identified at the time pelvic MR imaging is performed.

It is essential to accurately classify MDAs, as surgical planning often varies widely between MDA subtypes and can be driven by concomitant conditions or anatomic deformities (Table 2). If the classification is uncertain or multiple subtypes of MDA are present, it is best to describe the anomalies rather than forcing them into a class.

References

1. Troiano RN, McCarthy SM. Mullerian duct anomalies: imaging and clinical issues. Radiology 2004; 233(1):19–34.
2. Devi Wold AS, Pham N, Arici A. Anatomic factors in recurrent pregnancy loss. Semin Reprod Med 2006;24(1):25–32.
3. Li S, Qayyum A, Coakley FV, Hricak H. Association of renal agenesis and mullerian duct anomalies. J Comput Assist Tomogr 2000;24(6):829–834.
4. Pittock ST, Babovic-Vuksanovic D, Lteif A. Mayer-Rokitansky-Küster-Hauser anomaly and its associated malformations. Am J Med Genet A 2005;135 (3):314–316.
5. Oppelt P, Renner SP, Kellermann A, et al. Clinical aspects of Mayer-Rokitansky-Kuester-Hauser syndrome: recommendations for clinical diagnosis and staging. Hum Reprod 2006;21(3):792–797.
6. Kimberley N, Hutson JM, Southwell BR, Grover SR. Vaginal agenesis, the hymen, and associated anomalies. J Pediatr Adolesc Gynecol 2012;25(1):54–58.

Table 2
MDAs and Their Findings, Treatment, and Special Considerations

MDA Subtype	Uterine Findings	Associated Anomalies	Treatment	Special Considerations
Uterine agenesis or hypoplasia	Absent to very small uterus	Associated renal or ureteric anomalies in 40%	Isolated vaginal agenesis or atresia with a normal uterus may require surgery if amenorrhea, hematometra, or cyclic pelvic pain is present	Sagittal plane imaging is key to assessing extent of vaginal agenesis
Unicornuate uterus	Typically single uterine horn with or without a small rudimentary horn	Ipsilateral renal anomalies in 40% (typically renal agenesis)	A rudimentary horn with functional endometrium may require surgery	If a rudimentary horn is present, evaluate for endometrium
Uterus didelphys	Two widely divergent uterine horns and a deep external fundal cleft (>1 cm)	High association between obstructed hemivagina and ipsilateral renal agenesis	Vaginal obstruction may manifest shortly after menarche, lead to complications, and require intervention	True coronal imaging essential to evaluate for a uterine fundal cleft
Bicornuate uterus	Deep external fundal cleft (>1 cm); two separate endometrial canals communicate	Longitudinal vaginal septum in 25%	Surgery usually not indicated	True coronal imaging essential to evaluate for a uterine fundal cleft; may be unicollis or bicollis
Septate uterus	Convex or minimally indented (<1 cm) external fundal contour	None	Surgical resection may be considered if recurrent fetal loss occurs	Important to assess for muscular or fibrous components of the septum
Arcuate uterus	Normal external fundal contour; mild, broad-based inward contour of the endometrium at the fundus	None	Usually none unless recurrent fetal loss occurs	None
DES uterus	T-shaped configuration of uterus, narrowed fundus	Fallopian tubes often truncated	None	Increased prevalence of vaginal clear cell carcinoma

7. Gell JS. Müllerian anomalies. Semin Reprod Med 2003;21(4):375–388.
8. Buttram VC Jr, Gibbons WE. Müllerian anomalies: a proposed classification. (An analysis of 144 cases.) Fertil Steril 1979;32(1):40–46.
9. The American Fertility Society classifications of adnexal adhesions, distal tubal occlusion, tubal occlusion secondary to tubal ligation, tubal pregnancies, müllerian anomalies and intrauterine adhesions. Fertil Steril 1988;49(6):944–955.
10. Deutch TD, Abuhamad AZ. The role of 3-dimensional ultrasonography and magnetic resonance imaging in the diagnosis of müllerian duct anomalies: a review of the literature. J Ultrasound Med 2008;27(3):413–423.
11. Bermejo C, Martínez Ten P, Cantarero R, et al. Three-dimensional ultrasound in the diagnosis of Müllerian duct anomalies and concordance with magnetic resonance imaging. Ultrasound Obstet Gynecol 2010;35(5):593–601.
12. Mueller GC, Hussain HK, Smith YR, et al. Müllerian duct anomalies: comparison of MRI diagnosis and clinical diagnosis. AJR Am J Roentgenol 2007;189(6):1294–1302.
13. Robbins JB, Parry JP, Guite KM, et al. MRI of pregnancy-related issues: müllerian duct anomalies. AJR Am J Roentgenol 2012;198(2):302–310.
14. Olpin JD, Heilbrun M. Imaging of müllerian duct anomalies. Clin Obstet Gynecol 2009;52(1):40–56.
15. Chan YY, Jayaprakasan K, Zamora J, Thornton JG, Raine-Fenning N, Coomarasamy A. The prevalence of congenital uterine anomalies in unselected and high-risk populations: a systematic review. Hum Reprod Update 2011;17(6):761–771.
16. Grimbizis GF, Camus M, Tarlatzis BC, Bontis JN, Devroey P. Clinical implications of uterine malformations and hysteroscopic treatment results. Hum Reprod Update 2001;7(2):161–174.
17. Acién P. Incidence of müllerian defects in fertile and infertile women. Hum Reprod 1997;12(7):1372–1376.
18. Yoder IC, Hall DA. Hysterosalpingography in the 1990s. AJR Am J Roentgenol 1991;157(4):675–683.

19. Krysiewicz S. Infertility in women: diagnostic evaluation with hysterosalpingography and other imaging techniques. AJR Am J Roentgenol 1992;159(2): 253–261.

20. Chandler TM, Machan LS, Cooperberg PL, Harris AC, Chang SD. Mullerian duct anomalies: from diagnosis to intervention. Br J Radiol 2009;82(984): 1034–1042.

21. Miller RJ, Breech LL. Surgical correction of vaginal anomalies. Clin Obstet Gynecol 2008;51(2): 223–236.

22. Blask AR, Sanders RC, Rock JA. Obstructed uterovaginal anomalies: demonstration with sonography. II. Teenagers. Radiology 1991;179(1):84–88.

23. Strübbe EH, Willemsen WN, Lemmens JA, Thijn CJ, Rolland R. Mayer-Rokitansky-Küster-Hauser syndrome: distinction between two forms based on excretory urographic, sonographic, and laparoscopic findings. AJR Am J Roentgenol 1993;160 (2):331–334.

24. Rosenberg HK, Sherman NH, Tarry WF, Duckett JW, Snyder HM. Mayer-Rokitansky-Kuster-Hauser syndrome: US aid to diagnosis. Radiology 1986;161 (3):815–819.

25. Uğur M, Turan C, Mungan T, et al. Endometriosis in association with müllerian anomalies. Gynecol Obstet Invest 1995;40(4):261–264.

26. Olive DL, Henderson DY. Endometriosis and mullerian anomalies. Obstet Gynecol 1987;69(3 pt 1): 412–415.

27. Jayasinghe Y, Rane A, Stalewski H, Grover S. The presentation and early diagnosis of the rudimentary uterine horn. Obstet Gynecol 2005;105(6): 1456–1467.

28. Fedele L, Dorta M, Brioschi D, Villa L, Arcaini L, Bianchi S. Re-examination of the anatomic indications for hysteroscopic metroplasty. Eur J Obstet Gynecol Reprod Biol 1991;39(2):127–131.

29. Fedele L, Bianchi S, Marchini M, Mezzopane R, Di Nola G, Tozzi L. Residual uterine septum of less than 1 cm after hysteroscopic metroplasty does not impair reproductive outcome. Hum Reprod 1996; 11(4):727–729.

30. Carrington BM, Hricak H, Nuruddin RN, Secaf E, Laros RK Jr, Hill EC. Müllerian duct anomalies: MR imaging evaluation. Radiology 1990;176(3): 715–720.

31. Pellerito JS, McCarthy SM, Doyle MB, Glickman MG, DeCherney AH. Diagnosis of uterine anomalies: relative accuracy of MR imaging, endovaginal sonography, and hysterosalpingography. Radiology 1992;183(3):795–800.

32. Sarto GE, Simpson JL. Abnormalities of the müllerian and wolffian duct systems. Birth Defects Orig Artic Ser 1978;14(6C):37–54.

33. Ott DJ, Fayez J, Zagoria R, eds. Congenital anomalies. In: Hysterosalpingography: a text and atlas. 2nd ed. Philadelphia, Pa: Lippincott Williams & Wilkins, 1998; 59–69.

34. Zanetti E, Ferrari LR, Rossi G. Classification and radiographic features of uterine malformations: hysterosalpingographic study. Br J Radiol 1978;51(603): 161–170.

35. Fedele L, Dorta M, Brioschi D, Massari C, Candiani GB. Magnetic resonance evaluation of double uteri. Obstet Gynecol 1989;74(6):844–847.

36. Rackow BW, Arici A. Reproductive performance of women with müllerian anomalies. Curr Opin Obstet Gynecol 2007;19(3):229–237.

37. Homer HA, Li TC, Cooke ID. The septate uterus: a review of management and reproductive outcome. Fertil Steril 2000;73(1):1–14.

38. Raga F, Bauset C, Remohi J, Bonilla-Musoles F, Simón C, Pellicer A. Reproductive impact of congenital müllerian anomalies. Hum Reprod 1997;12 (10):2277–2281.

39. Fedele L, Bianchi S. Hysteroscopic metroplasty for septate uterus. Obstet Gynecol Clin North Am 1995;22(3):473–489.

40. Fayez JA. Comparison between abdominal and hysteroscopic metroplasty. Obstet Gynecol 1986;68(3): 399–403.

41. Propst AM, Hill JA 3rd. Anatomic factors associated with recurrent pregnancy loss. Semin Reprod Med 2000;18(4):341–350.

42. Zreik TG, Troiano RN, Ghoussoub RA, Olive DL, Arici A, McCarthy SM. Myometrial tissue in uterine septa. J Am Assoc Gynecol Laparosc 1998;5(2): 155–160.

43. Reuter KL, Daly DC, Cohen SM. Septate versus bicornuate uteri: errors in imaging diagnosis. Radiology 1989;172(3):749–752.

44. Fedele L, Ferrazzi E, Dorta M, Vercellini P, Candiani GB. Ultrasonography in the differential diagnosis of "double" uteri. Fertil Steril 1988;50(2): 361–364.

45. Tulandi T, Arronet GH, McInnes RA. Arcuate and bicornuate uterine anomalies and infertility. Fertil Steril 1980;34(4):362–364.

46. Herbst AL, Ulfelder H, Poskanzer DC. Adenocarcinoma of the vagina: association of maternal stilbestrol therapy with tumor appearance in young women. N Engl J Med 1971;284(15):878–881.

47. Kaufman RH, Adam E, Binder GL, Gerthoffer E. Upper genital tract changes and pregnancy outcome in offspring exposed in utero to diethylstilbestrol. Am J Obstet Gynecol 1980;137(3):299–308.

48. Goldberg JM, Falcone T. Effect of diethylstilbestrol on reproductive function. Fertil Steril 1999;72(1): 1–7.

49. Ansbacher R. Uterine anomalies and future pregnancies. Clin Perinatol 1983;10(2):295–304.

50. DeCherney AH, Cholst I, Naftolin F. Structure and function of the fallopian tubes following exposure to diethylstilbestrol (DES) during gestation. Fertil Steril 1981;36(6):741–745.

51. Rennell CL. T-shaped uterus in diethylstilbestrol (DES) exposure. AJR Am J Roentgenol 1979;132 (6):979–980.

52. Kipersztok S, Javitt M, Hill MC, Stillman RJ. Comparison of magnetic resonance imaging and transvaginal ultrasonography with hysterosalpingography in the evaluation of women exposed to diethylstilbestrol. J Reprod Med 1996;41(5):347–351.

53. Salle B, Sergeant P, Awada A, et al. Transvaginal ultrasound studies of vascular and morphological changes in uteri exposed to diethylstilbestrol in utero. Hum Reprod 1996;11(11):2531–2536.

54. van Gils AP, Tham RT, Falke TH, Peters AA. Abnormalities of the uterus and cervix after diethylstilbestrol exposure: correlation of findings on MR and hysterosalpingography. AJR Am J Roentgenol 1989;153(6):1235–1238.

Imaging of Müllerian Duct Anomalies

Spencer C. Behr, MD • Jesse L. Courtier, MD • Aliya Qayyum, MBBS

Page E235

While the presence of a divided rather than triangular uterine cavity at HSG may suggest the presence of an MDA, it is not possible to differentiate between subtypes. MR imaging and US provide greater anatomic detail; both of these imaging methods provide information on the external uterine contour, which is an important diagnostic feature of MDAs. Furthermore, both MR imaging and US may be used to assess for concomitant renal anomalies; renal anomalies occur at a higher rate among MDA patients.

Page E240

A further important advantage of MR imaging is the ability to readily evaluate the patient for concurrent renal anomalies, reported to occur in approximately 40% (30%–50%) of patients with MDAs.

Page E241

However, the presence of endometrium in a rudimentary horn is an important finding and should be reported. Endometrial tissue in a noncommunicating rudimentary horn can manifest clinically with pelvic pain caused by the increased prevalence of endometriosis due to retrograde flow of menses through the obstructed horn or due to an obstructed, distended horn.

Page E244

A fundal cleft greater than 1 cm has been reported to be 100% sensitive and specific in differentiation of fusion anomalies (didelphys and bicornuate) from reabsorption anomalies (septate and arcuate).

Page E247

It is important to identify myometrium versus fibrous tissue within the septum, since the surgical approach differs for the two entities; while a less invasive hysteroscopic septoplasty can be used to treat a fibrous septum, a transabdominal surgical approach is required for treatment of a muscular septum.